

Department of Electrical & Systems Engineering

Departmental Papers (ESE)

University of Pennsylvania

Year 2001

Electromagnetic wave propagation in the
wire medium: a complex medium with
long thin inclusions

Charles Anthony Moses*

Nader Engheta†

*University of Pennsylvania

†University of Pennsylvania, engheta@ee.upenn.edu

Postprint version. Published in *Wave Motion*, Volume 34, Issue 3, September 2001, pages 301-317.

Publisher URL: [http://dx.doi.org/10.1016/S0165-2125\(01\)00095-6](http://dx.doi.org/10.1016/S0165-2125(01)00095-6)

This paper is posted at ScholarlyCommons.

http://repository.upenn.edu/ese_papers/280

Electromagnetic Wave Propagation in the Wire Medium: A Complex Medium with Long Thin Inclusions

C. A. Moses and N. Engheta

Moore School of Electrical Engineering

University of Pennsylvania, Philadelphia, PA 19104

September 10, 2000

Abstract

The wire medium is a type of complex artificial material we conceptually envision as many identical finite-length, parallel, thin wire inclusions embedded within a host medium. It is representative of a class of novel artificial materials characterized by long thin inclusions. Unlike some conventional artificial material, the inclusions of this class are not necessarily electrically short. Here we present our theoretical analysis for wire media and, by studying certain salient features of plane wave propagation through these media, introduce equivalent medium parameters that depend, among other parameters, on the direction of wave propagation. The approach we use separates the artificial material into its elementary planes and then uses periodic moment method techniques to individually characterize each elementary plane. Analytic formulas from periodic structure theory are then used to determine the effective wavenumber for the overall medium and the transverse impedance at the midpoint between adjacent elementary planes. Our examples show that some realizations of these media are spatially dispersive and may exhibit interesting features such as “angular windows of propagation” and other properties that are dependent on the polarization, frequency, and direction of wave propagation.

1 Introduction

The history of artificial materials seems to date back to the pioneering work of Lindman (for review, see [1]) who, in 1914, fabricated a chiral medium from a collection of randomly-oriented small wire helices. Kock [2] later suggested that a large-scale model of a solid dielectric, with small metallic inclusions playing the role of the molecules of the dielectric, might duplicate some of a solid dielectric's essential macroscopic electromagnetic features. As a demonstration of their practical use, Kock fabricated lightweight microwave lenses from periodic arrangements of conducting spheres, disks, and strips, and in doing so, verified his predictions for modification of the effective refractive index of the artificial material. Kock's theory, like many of its modern-day counterparts, utilizes a low frequency, quasi-static analysis to determine the polarizability of each inclusion. Once the polarizabilities are known, spatial averaging establishes the effective net polarization and magnetization of the bulk artificial material. The similarity to real dielectrics then permits one to ascribe to the artificial material an effective permittivity and permeability, an estimate of which may be determined by means of Lorentz's theory for non-polar dielectrics [3, Sec. 8-1] or other well-known mixing formulas [4]. An interesting point noted by Brown [5] in his review on artificial dielectrics is that Kock's theory essentially "returns to the starting point of classical dielectric theory, since Mossotti developed his theory by postulating that a solid dielectric could be represented as a lattice of conducting spheres."

The investigation of artificial and complex materials is not merely of academic interest; analysis of wave propagation through artificial materials is necessary in connection with their use in fabricating some special microwave devices (for examples, see [5]). In principle, devices fabricated using real material for application at optical frequencies may be designed for lower frequency (e.g., microwave) using artificial material by simply length scaling all dimensions (e.g., see [6]). In this regard, it is of no surprise that a recent push toward integrating the concepts of solid state physics with artificial materials has brought forth new ideas and applications for artificial materials (e.g., 3D wire mesh photonic crystals [7]). In comparison to some solid dielectrics, an artificial dielectric may feature low density and may offer significant cost and weight

savings [8].

Recent research efforts in designing artificial complex material have introduced some unusual inclusions intended to achieve interesting electromagnetic features; as an example, inclusions intended to produce artificial material with similar characteristics as optically active (chiral) media have received much attention (e.g., [9, 10, 11]). Along with advances in inclusion design, researchers have proffered improved polarizability models (e.g., [12, 13, 14, 15, 16, 17]) and mixing formulas (e.g., [18, 19, 20, 21]). But without combining these two steps into a single step, the same fundamental theoretical limitations [22, p. 751] on inclusion size and density encountered by Kock in his modeling also limit modeling more general media.

To circumvent these limitations all at once, an entirely numerical procedure based on the method of moments was proposed by Blanchard, Newman and Peters [23] and Newman and Peters [24] for analyzing artificial material with inclusions distributed about a periodic lattice (they illustrate their technique for an infinite artificial medium composed of closely-spaced, short, conducting wires and wire crosses). Unlike conventional analytic techniques, their approach has the advantage of directly taking into account all of the mutual coupling effects between inclusions, regardless of their size, shape, orientation, or composition, so long as all the inclusions are identical. In the course of analysis, however, the elements of the moment method impedance matrix must be determined by evaluating a conditionally-convergent triply-infinite sum. Supposing the necessary acceleration techniques (e.g., see [25]) are used for computing the sum, the propagation constants for plane wave propagation in a specified direction may then be found by requiring the determinant of the impedance matrix to vanish. Since the elements of the impedance matrix themselves depend upon the wavenumber, the process is iterative and may be computationally demanding.

Traditionally, in the analysis of the electromagnetic properties of complex media, more attention has been given to cases where the inclusions, which are dispersed in some manner throughout the host media, are assumed to be small compared to the wavelength (i.e., they are electrically small). However, can one imagine a novel class of artificial materials in which the inclusions are permitted to be electrically long in one dimension, but still electrically small in the other two dimensions (i.e., they have small transverse cross sections that might vary along the length of an inclusion, but at every point along the major axis of this

inclusion the transverse cross section would be axially symmetric)? These inclusions can then all be positioned in parallel and in close proximity to each other so the entire structure can be viewed macroscopically as a *medium*. How might one analyze wave propagation in such a medium?

As is well known, the electromagnetic description of media is generally rendered macroscopically through constitutive relations expressed by $\mathcal{D} = \epsilon_o \mathcal{E} + \mathcal{P}$ and $\mathcal{H} = \frac{1}{\mu_o} \mathcal{B} - \mathcal{M}$ where the field vectors take their usual meanings, \mathcal{P} and \mathcal{M} are the polarization and magnetization, respectively, (in principle \mathcal{P} and \mathcal{M} may include higher-order multipoles as well as dipole moments) and the constants ϵ_o and μ_o are, respectively, the permittivity and permeability of vacuum. In general, \mathcal{P} and \mathcal{M} may be functions of both \mathcal{E} and \mathcal{B} , as they are, for example, in bi-anisotropic and bi-isotropic (i.e., chiral) media (e.g., see [9]). For media that may be conductive, one can also have $\frac{\partial}{\partial t} \mathcal{D} = \epsilon_o \frac{\partial}{\partial t} \mathcal{E} + \mathcal{J}_e$ to indicate the presence of an induced electric current \mathcal{J}_e . Obviously, if one sets $\mathcal{J}_e = \partial \mathcal{P} / \partial t$, then the first and third equations above are mathematically equivalent in non-static conditions. Therefore, one could mathematically absorb \mathcal{J}_e into \mathcal{P} (or vice versa); however, the decision to use \mathcal{J}_e alone, \mathcal{P} alone, or both \mathcal{J}_e and \mathcal{P} to describe induced electric effects is usually based on physical knowledge of the microscopic structure of the material. For example, an artificial material with electrically short inclusions might be best described through \mathcal{P} since in such media one can readily identify the induced electric dipoles (the magnetic dipoles can be handled by means of \mathcal{M}). Similarly, a theory for a material with infinitely-long conductive fibers (that is applicable to the case of the rodged media described by Brown [26], for example) might permit unimpeded induced current and would be best described through \mathcal{J}_e . We propose that media with long (but not infinitely-long) thin inclusions (as we have mentioned in the preceding paragraph) might be best modeled by means of both \mathcal{P} and \mathcal{J}_e ; the effects due to the long dimension of the inclusions can be modeled through \mathcal{J}_e , whereas the effects due to the small cross section in the other two dimensions can be handled using \mathcal{P} and/or \mathcal{M} (including higher-order multipoles as appropriate). For media in which \mathcal{P} and \mathcal{J}_e both contribute to the induced effects, the

Maxwell equations—when combined with the constitutive relations—can be written as:

$$\nabla \times \boldsymbol{\mathcal{E}} + \frac{\partial}{\partial t} \boldsymbol{\mathcal{B}} = 0 \quad (1a)$$

$$\frac{1}{\mu_o} \nabla \times \boldsymbol{\mathcal{B}} - \epsilon_o \frac{\partial}{\partial t} \boldsymbol{\mathcal{E}} = \boldsymbol{\mathcal{J}}_s + \boldsymbol{\mathcal{J}}_e + \frac{\partial}{\partial t} \boldsymbol{\mathcal{P}} + \nabla \times \boldsymbol{\mathcal{M}} \quad (1b)$$

with $\boldsymbol{\mathcal{J}}_e^{\text{total}} = \boldsymbol{\mathcal{J}}_e + \frac{\partial}{\partial t} \boldsymbol{\mathcal{P}}$ representing the total induced current within the medium and $\boldsymbol{\mathcal{J}}_s$ representing the source (if any).

In the present paper, we discuss wave propagation in a special illustrative example of this novel class of artificial material. The example that we discuss can be envisioned as a three-dimensional periodic artificial medium conceptually synthesized by embedding many identical, finite-length, parallel thin wires within some host material. Unlike conventional artificial complex media for which the inclusions are typically electrically short, the wire inclusions in these media need not necessarily be small compared to the wavelength. The wires can be chosen, per design, to have a length from a fraction of a wavelength to multiple wavelengths. However, the spatial periodicities¹ in such media are still chosen to be (electrically) small so an ensemble of such wires would have the macroscopic characteristics of a *medium* and would inhibit the well known grating-lobe and band-gap phenomena usually associated with periodic media. We have given such media the name *Wire Media*. The thin wire inclusion used in these media is an example of an inclusion that may be electrically long in one direction (i.e., length of the wire), but small in the other two dimensions (thin cross section). To examine propagation in these media, the electric current $\boldsymbol{\mathcal{J}}_e$ induced along each wire needs to be evaluated, whereas the polarization $\boldsymbol{\mathcal{P}}$ and magnetization $\boldsymbol{\mathcal{M}}$ (including multipole moments) induced due to the transverse cross section of the wire can be assumed to be negligibly small because the wire is taken to be thin². If the wire inclusions are attached to some end-elements (as in the case of FFFB media [27]), then $\boldsymbol{\mathcal{P}}$ and/or $\boldsymbol{\mathcal{M}}$ induced due to the presence of the end-elements needs to

¹The periodicities mentioned above are not necessarily essential to constructing a wire medium; however, here we introduce them to simplify the electromagnetic analysis. Generally, one may place the wires randomly, but all parallel with some fixed orientation and an average inter-element spacing related to the spacings of the periodic media. This has not been investigated here.

²If a more exact model is desired, the polarization and magnetization (and higher-order multipoles, as needed) induced due to the transverse cross sections of the wires can be evaluated based on a quasi-static approach. However, for the media presented here, these effects would be negligible.

be analyzed independently.

Our approach is intermediary to the completely numerical approach of Blanchard, Newman, and Peters and the completely analytical quasi-static technique of Kock. Instead of either of these approaches, we use a combination of both analytical and numerical techniques to analyze some of the salient features of plane wave propagation in wire media. Specifically, we blend the technique used by Brown [26] of breaking an artificial material into its *elementary planes* with Blanchard *et al.*'s periodic moment method approach (applied only for a single elementary plane rather than the entire medium). By treating the three-dimensional artificial material as a concatenation of many closely-spaced elementary planes (each of which contains inclusions located on a two-dimensional periodic lattice), the numerical calculations can be focused on characterizing one elementary plane completely, since well-known analytical formulas can be used under certain circumstances to describe the interaction of many identical elementary planes if the characteristics of a single plane are known.

If the elementary planes are periodically spaced, then the currents induced on inclusions in any single plane are related to those in any other by only a multiplicative complex factor that may be determined by means of Floquet's theory [22, Sec. 9.1]. When an incident plane wave illuminates one elementary plane, to solve for the currents induced on the inclusions of that plane, one can use the periodic moment method technique [28] and apply the Poisson sum formula [3, Sec. 11-9] to write the appropriate Green's function appearing in the integral equation as a rapidly converging series (as previously reported by Munk and Burrell [29] in the analysis of super-dense dipole arrays). If the two-dimensional lattice period on each elementary plane is small enough, then only one scattered wave propagates away from the plane (into each half-space separated by the plane); that is, there are no grating lobes. The appropriate coefficient of the scattered wave is proportional to some properly defined *average* current induced in that plane, suggesting that we might replace the actual current distribution on each plane by this average value (together with the appropriate phase variations as determined by the angle of incidence of the incident wave). Conceptually, the elementary plane is being replaced by a thin admittance sheet with an admittance equal to the ratio of the average current to the average total tangential electric field on the plane. Based on this equivalent

admittance sheet, we then treat the three-dimensional artificial material as if it were fabricated from periodic spacings of admittance sheets and reformulate the problem as a periodically loaded transmission line problem. By doing so, we neglect entirely all the evanescent waves excited by the currents in each elementary plane; clearly this neglect is permissible only if the evanescent waves of one elementary plane have sufficiently decayed before reaching the next elementary plane³. If so, then well-known periodic structure theory [30, Chp. 8] may be used to determine the wavenumber and transverse impedance associated with the lowest-order wave in this artificial material. Under certain conditions, the overall structure *effectively* acts as an artificial medium, with some equivalent effective (tensorial) permittivity. On the other hand, the permeability of the artificial material is taken to be that of vacuum, since: (1) the wires are non-magnetic; (2) the wires are very thin, so there is little opportunity to develop significant eddy-currents on any one wire; and (3), the volume density is very low (see Footnote 2). Since our technique completely evaluates the mutual coupling between neighboring inclusions in any single elementary plane, it follows that no electromagnetic modeling limitations are placed on the lengths of the wires, provided the spacing between planes is chosen properly (see Footnote 3). Our investigation of these media shows that a variety of polarization, frequency, and angle of propagation dependencies may be engineered into a wire medium by judiciously choosing the lengths and separations of the wires in each plane, as well as the interplanar spacings. Furthermore, with the additional degrees of freedom that these media possess, the observation of Blanchard, *et al.*, that “one may be able to engineer or design a medium which has desirable permeability, permittivity, and dispersion characteristics” appears to be even more viable [23].

Our interest in studying wire media was brought about by our theoretical research on plane-wave propagation in artificial feedforward-feedbackward (FFFB) media [31, 27, 32]. In the conceptualization of FFFB media, a large number of small inclusions were dispersed throughout some host material (as in conventional artificial material) and then pairs of inclusions were connected by means of tiny⁴ transmission lines. In such a conceptualization of FFFB media, all of the transmission lines were parallel. As would be ex-

³ More will be said about this matter later in this paper.

⁴The adjective *tiny* refers to the cross-sectional area, not length, of the connecting transmission lines. In our conceptualization of FFFB media, the tiny-transmission lines may be of any length.

pected, plane wave propagation in the axial direction (i.e., along the direction of the transmission line axis) of FFFB media requires knowledge of only the transverse characteristics of the medium since the electromagnetic waves cannot significantly interact *directly* with the transmission line [27]. However, for oblique propagation, the wave may suffer significant interaction with these transmission lines, and, therefore, may induce currents and charge separations directly on the transmission lines. To understand these interactions and to simplify the analysis, we can conceptually replace the two-wire transmission lines with single wires of equivalent radius. Such wires, without the end-elements attached, are the constituent inclusions of wire media, as addressed above.

2 Single elementary plane analysis

The types of surfaces resembling the elementary planes in wire media have been called Super-Dense Dipole surfaces (or Gangbuster surfaces) by Schneider and Munk [33], Larson and Munk [34], and Kornbau [35]. The labels *super-dense* and *gangbuster* refer to the feature that the wire lengths may be greater than the lattice periodicity (accomplished by tilting the wire axes away from one lattice axis; see Figure 1). One of the underlying motivations for study of Super-Dense surfaces is due to their application as broad-band frequency selective surfaces (FSS) and polarization selective surfaces [33]. Noted investigations of these surfaces have utilized elements excited at or below their first resonance frequency, but there seems to be no theoretical or practical limitations that would prohibit longer elements.

The fundamental research on bi-infinite arrays with arbitrarily oriented piece-wise linear elements (from which the theory of gangbuster surfaces originates) was performed by Munk and Burrell [29]; here we present only a brief summary of their work, but please note a slight change of notation. Consider the array illustrated in Figure 2 where the (l, m) th cylindrical wire element lies in the τ - ζ (or y - z) plane with center at $(\tau, \zeta) = (lD_\tau, mD_\zeta)$ and with its axis tilted away from the ζ -axis by some angle α (note: the axes of the wires are aligned with the z -axis). The value of α for square (i.e., $D_\tau = D_\zeta = D$) gangbuster dipole surfaces is constrained by $\alpha = \arctan(1/\bar{n})$, where \bar{n} is some integer [33]; simply stated, a type \bar{n} gangbuster



Figure 1: An example gangbuster surface. In this illustration, the radius of the dipoles is exaggerated five times in order to be visible in print. The parameters $D = 0.13\Lambda$, $L = 0.533\Lambda$, $a = 0.001\Lambda$, and $n = 4$ were used to construct this surface (see text and Figure 2 for parameter explanations). From these parameters, one can compute $\alpha = 14.0^\circ$, $d_{\text{near}} = 0.0315\Lambda$, and $d_{\text{end}} = 0.006\Lambda$. Here Λ is some reference length that may be chosen to scale this surface to any desired physical dimension.

dipole surface has the property that the midpoints of two neighboring collinear wire elements are separated by \bar{n} periodicity units along one axis and one periodicity unit along the perpendicular axis. As shown in Figure 2, each wire has overall length L and radius a ; simple geometrical relations show the nearest parallel wires to be separated by $d_{\text{near}} = (L + d_{\text{end}})/(1 + \bar{n}^2)$, where d_{end} is the distance between ends of any two neighboring collinear wires. An example of a gangbuster surface is shown in Figure 1. The parameters used to create this surface are listed in Figure 1, where Λ is some reference length that may be assigned any desired value; it is independent of the wavelength of the incident wave in the host medium which we designate as λ_o . The surface shown in the figure measures $0.7\Lambda \times 0.7\Lambda$.

Suppose the array is illuminated by a plane wave $\mathbf{E}^{(\text{inc})} = \mathbf{E}_o e^{-jk_o \hat{\mathbf{s}} \cdot \mathbf{r}}$ (an $e^{j\omega t}$ time-dependence is implicit throughout) propagating in the direction of the unit vector $\hat{\mathbf{s}} = s_x \hat{\mathbf{x}} + s_y \hat{\mathbf{y}} + s_z \hat{\mathbf{z}}$, where $k_o = \omega \sqrt{\mu_o \epsilon_o} = 2\pi/\lambda_o$, then, as one might expect, only the portion of this wave TM^z polarized appreciably interacts with the wire elements (the TE^z portion has no electric field component parallel to the wires). In terms of the the incident electric field, the TM^z portion is $\mathbf{E}^{(\text{inc}), \text{TM}} = (\hat{\mathbf{z}} \cdot \mathbf{E}_o) \left(\hat{\mathbf{z}} - \frac{\mathbf{s}_t s_z}{1 - s_z^2} \right) e^{-jk_o \hat{\mathbf{s}} \cdot \mathbf{r}}$; here $\mathbf{s}_t = \hat{\mathbf{s}} - \hat{\mathbf{z}} s_z$ is

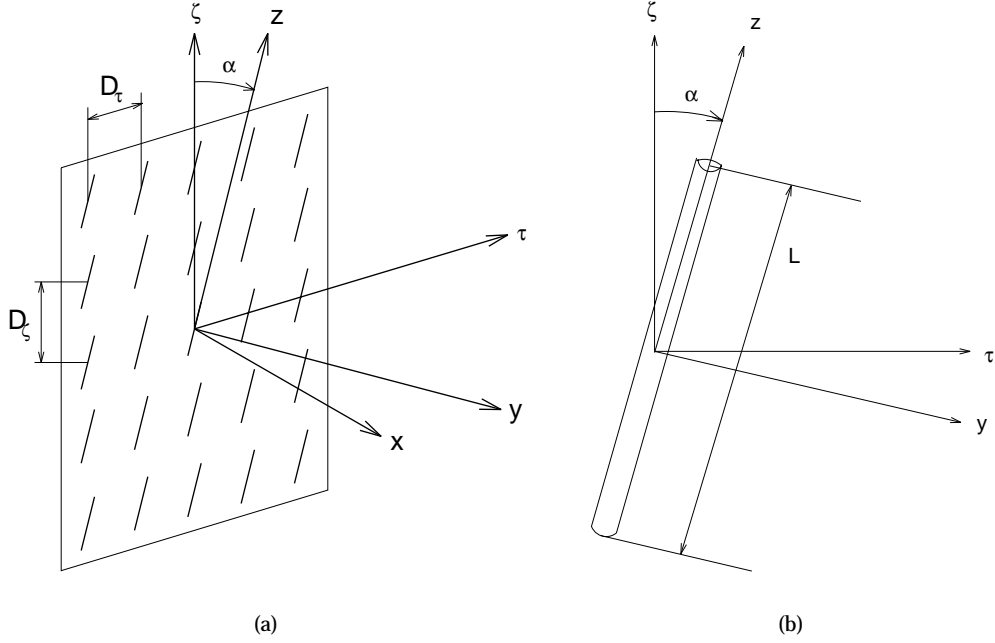


Figure 2: (a) The bi-infinite wire array as an elementary plane and (b) one wire element.

the transverse (to z) part of \hat{s} . If the elements are sufficiently thin, azimuthally symmetric surface currents will be induced on the periphery of each wire. For our purposes, the surface current can be replaced by a filament of current, $I(z)$, lying along the axis of each wire. As derived by Munk and Burrell [29], the electric field at an observation point $\mathbf{r} = (x, y, z)$ exterior to the array is given by

$$\mathbf{E}^{(\text{scat})} = \frac{\eta_o}{2D_\tau D_\zeta} \sum_{h=-\infty}^{+\infty} \sum_{n=-\infty}^{+\infty} \mathbf{e}_\pm \frac{e^{-jk_o(\mathbf{r}-\mathbf{r}_o)\cdot\mathbf{r}_\pm}}{r_x} \int_{-L/2}^{+L/2} I(z') e^{+jk_o z' \hat{z}\cdot\mathbf{r}_\pm} dz' \quad x \geq x_o \quad (2)$$

where η_o is the intrinsic impedance of the surrounding medium, k_o is the wavenumber associated with a plane wave in the surrounding medium, $\mathbf{r}_o = (x_o, y_o, z_o)$ is a reference point taken to be the midpoint of the reference dipole element on the surface, and: $r_x = \sqrt{1 - \left(s_\tau + h \frac{\lambda_o}{D_\tau}\right)^2 - \left(s_\zeta + n \frac{\lambda_o}{D_\zeta}\right)^2}$, $\mathbf{r}_\pm = \pm \hat{x} r_x + \hat{\tau} \left(s_\tau + h \frac{\lambda_o}{D_\tau}\right) + \hat{\zeta} \left(s_\zeta + n \frac{\lambda_o}{D_\zeta}\right)$, and $\mathbf{e}_\pm = (\hat{z} \times \mathbf{r}_\pm) \times \mathbf{r}_\pm$. As can be seen, r_x , \mathbf{r}_\pm , and \mathbf{e}_\pm take the summation indices h and n as parameters. The choice of sign is made throughout depending upon the position of the observation point relative to the reference point ($x \geq x_o$). Note that the array lies in the $x = x_o$ plane. In

(2), $I(z)$ is the current distribution on the reference wire; the currents on all the other wires of the array are related to $I(z)$ by a complex factor in accordance with Floquet's theory: $I_{lm}(\tilde{z}) = I(\tilde{z})e^{-jk_o(lD_\tau s_\tau + mD_\zeta s_\zeta)}$. Here, $I_{lm}(\tilde{z})$ is the current on the (l, m) th wire and \tilde{z} is the local coordinate variable along that wire. The integral in (2) can be interpreted as the far-field pattern of a single element (without the obliquity factor) carrying a current distribution $I(z)$.

Each of the (h, n) terms in the summation corresponds to a Floquet spatial harmonic, and physically represents either an evanescent or propagating plane wave, depending upon the sign of r_x^2 ; if \mathbf{E}^{scat} is to be evaluated at a distance $|x - x_o|$ from the array, some of these terms may be neglected. The $h = n = 0$ term always propagates; it corresponds to the specular rays in the directions $\pm s_x \hat{x} + s_y \hat{y} + s_z \hat{z}$. If certain conditions are met on the periodicity of the array in the τ and ζ directions ($D_\tau < \lambda_o/2$ and $D_\zeta < \lambda_o/2$), then no grating lobes are present and the specular wave is the only propagating scattered wave (for any angle of incidence); the electric field associated with the specular wave is determined by evaluating

$$\mathbf{E}^{(\text{spec})} = \frac{\eta_o \mathbf{e}_\pm e^{-jk_o(\mathbf{r}-\mathbf{r}_o)\cdot\mathbf{r}_\pm}}{2D_\tau D_\zeta \sqrt{1-s_\tau^2-s_\zeta^2}} \int_{-L/2}^{+L/2} I(z') e^{+jk_o z'(s_\tau \sin \alpha + s_\zeta \cos \alpha)} dz' \quad (3)$$

once the current distribution $I(z)$ is known on the reference element.

One can apply a moment method (MoM) procedure to determine the unknown current distribution and solve by matrix methods. In view of the relative simplicity of the anticipated current distribution, the unknown current can be expanded in terms of a complete set of entire domain basis functions consisting of even and odd modes that each vanish at each end of the wire: $I(z) = \sum_{p=1}^P I_p^e \cos[(2p-1)\frac{\pi z}{L}] + \sum_{q=1}^Q I_q^o \sin[q\frac{\pi z}{L}]$. After the current is expressed analytically, albeit with unknown modal coefficients, the integrals involving the current distribution appearing in (2) can be computed in closed form [32]. In usual moment method fashion, the unknown current coefficients are determined by requiring the total (incident plus scattered) tangential electric field to vanish on the surface of each wire element. In our work we have employed a Galerkin procedure with weighted residuals (e.g., see [36, Sec. 7.3]) and assumed azimuthal symmetry.

Once the current coefficients are known, the scattered field equations can be used to find the reflected TM^z wave. On defining the reflection coefficient⁵ as $\hat{R}_{\text{TM}} = E_z^{(\text{refl})} / E_z^{(\text{inc})}$, one finds

$$\hat{R}_{\text{TM}} = \frac{\eta_o L}{D_\tau D_\zeta} \frac{s_z^2 - 1}{\sqrt{1 - s_\tau^2 - s_\zeta^2}} \left\{ \sum_{p=1}^P \frac{I_p^e}{E_{oz}} \left\{ \text{sinc} \left[(2p-1) \frac{\pi}{2} - \frac{k_o L s_z}{2} \right] + \text{sinc} \left[(2p-1) \frac{\pi}{2} + \frac{k_o L s_z}{2} \right] \right\} + j \sum_{q=1}^Q \frac{I_q^o}{E_{oz}} \left\{ \text{sinc} \left[q\pi - \frac{k_o L s_z}{2} \right] + \text{sinc} \left[q\pi + \frac{k_o L s_z}{2} \right] \right\} \right\}. \quad (4)$$

Similarly, the corresponding transmission coefficient is $\hat{T}_{\text{TM}} = E_z^{(\text{tran})} / E_z^{(\text{inc})} = 1 + \hat{R}_{\text{TM}}$. The meaning of the hat over the coefficients will become apparent in the next section. We have not addressed the case of currents excited by TE^z waves because the electric field associated with these waves only develops a negligibly small charge separation across the diameter of the thin cylinders—not their length. Consequently, the elementary plane will be essentially transparent to TE^z waves.

3 Sheet admittance analogy

When a plane wave is used to illuminate a single gangbuster surface, one sees, at some distance from the surface, a reflected *plane* wave (assuming the surface is constructed to inhibit grating lobes). Since the reflected wave is planar, the array must effectively *appear* to carry some “average uniform surface current” (possibly with linearly progressive phase). This equivalent surface current is proportional to the specular reflection coefficient (not including certain obliquity factors). If we are only interested in the specular waves, we should be able to conceptually replace the elementary plane by an equivalent thin anisotropic admittance sheet that develops the same equivalent current. By doing so, we can simplify the analysis of the wire medium provided that the elementary planes are placed far enough apart so the first evanescent mode excited by one elementary plane is decayed sufficiently (say, at least 20 dB below the propagating mode [22, p. 773]) before reaching the next elementary plane and close enough so the periodicity is a small

⁵Since we are considering TM^z waves, all the field components can be derived from E_z ; therefore, the reflection coefficient, as it is defined here, is identical to one defined for the amplitude of the entire wave.

fraction of a wavelength. To determine the equivalent sheet admittance, we employ a general procedure involving the plane wave reflection coefficient. Based on this idea, we conceptually replace the gangbuster surface by a new surface—uniform in the z -direction—that develops the necessary equivalent surface current. If the new surface is taken to be an infinitesimally-thin anisotropic admittance sheet, then the induced current, which is restricted to flow along the axes of the wires (i.e., z -axis), is the product of the transverse admittance and the z -component of the total electric field: $\mathbf{J}_{\text{sh}} = \hat{z}Y_{\text{sh}}E_z$, where Y_{sh} is identified as the equivalent transverse sheet admittance. The electric field appearing here is the z -component of the total electric field. Clearly the necessary admittance will vary depending upon the parameters of the gangbuster surface; we shall show that it is also a function of the angle of incidence and frequency of the illuminating wave.

Suppose a plane-wave illuminates an impedance sheet lying in the $x = x_o$ plane. The usual boundary conditions hold for fields on opposite sides of the sheet: $\hat{x} \times (\mathbf{H}_2 - \mathbf{H}_1) = \mathbf{J}_{\text{sh}}$ and $\hat{x} \times (\mathbf{E}_2 - \mathbf{E}_1) = 0$. The subscript 1 refers to fields in the region $x < x_o$ and the subscript 2 refers to fields in the region $x > x_o$. An arbitrary plane wave propagating in the \hat{s} direction illuminates the sheet: $\mathbf{E}^{(\text{inc})} = \mathbf{E}_o e^{-jk_o \hat{s} \cdot \mathbf{r}}$. If we decompose the wave into TM^z and TE^z components, clearly the TE^z part, not having any \hat{z} -directed electric field component, cannot excite \mathbf{J}_{sh} ; for this reason we need only consider the TM^z portion, $\mathbf{E}^{(\text{inc}), \text{TM}}$. The reflected and transmitted waves, due to the TM^z incidence, will also be TM^z polarized. Satisfaction of the boundary conditions at the sheet permits solving for the unknown reflection and transmission coefficients R_{TM} and T_{TM} (we have assumed s_x positive):

$$R_{\text{TM}} = -1 \left/ \left[1 + \frac{2}{\eta_o Y_{\text{sh}}} \frac{-s_x}{1 - s_z^2} \right] \right. \quad T_{\text{TM}} = 1 \left/ \left[1 + \frac{\eta_o Y_{\text{sh}}}{2} \frac{1 - s_z^2}{-s_x} \right] \right. \quad (5)$$

Inverting the first relation to find $\eta_o Y_{\text{sh}} = \frac{-2R_{\text{TM}}}{1+R_{\text{TM}}} \frac{-s_x}{1-s_z^2}$. Since the wires in the gangbuster surface are presumed loss-less, we anticipate that the necessary admittance must be purely susceptive, with $Y_{\text{sh}} = jB_{\text{sh}}$. However, when we use the reflection coefficient as found numerically through the moment method analysis described earlier (Equation 4) in the above equation, we find that a small amount of real part is present

in Y_{sh} . Some additional investigation shows the error is systematic and results from assuming (in executing the numerical procedure) that the dipole currents lie as filaments on the wire axis (rather than as surface currents on the wire's periphery). As detailed in [32], analysis shows that a simple transformation of the computed reflection coefficient can be made so that, if used in the above formula, will yield a purely imaginary sheet admittance. If we denote the compensated reflection coefficient by R_{TM} , then the appropriate transformation, $R_{\text{TM}} = \frac{\hat{R}_{\text{TM}}}{1 + j \tan(k_o s_x a) (R_{\text{TM}} - 1)}$, shows that the systematic correction is *not* merely a phase factor, as one might have thought. Clearly, as $k_o s_x a$ reduces to zero, then the difference between the computed reflection coefficient and the compensated reflection coefficient vanishes. For electrically-thin wire inclusions, this factor, although very small, is non-negligible.

4 Transmission line analysis

Analysis of artificial material can make use of the similarity of plane wave propagation and wave propagation on TEM transmission lines [37]. In this context, the anisotropic sheet admittances introduced earlier are analogous to shunt admittances placed across a transmission line. Here we only consider TM^x plane waves, but the theory can be readily extended to include TE^z plane waves as another case. Suppose we take the position along the transmission line to correspond to the x variable of Cartesian space. Then, if we correspond the voltage on the transmission line with the total tangential electric field (E_z) and the current with the total tangential magnetic field ($\mp H_y$, for waves traveling in the $\pm \hat{x}$ direction), the characteristic impedance of the (unloaded, i.e., no shunt loading) line, $Z_{\text{TM}} = \eta_o \frac{1 - s_x^2}{s_x}$, can be found by taking the ratio of E_z to $-H_y$. The propagation constant on the (unloaded) line is $k_o s_x$. (In these equations we have taken the real part of s_x to be positive since we are considering propagation in the positive x direction.) Using this model, we can show that reflection from a shunt load Y_{sh} placed across the transmission line causes a wave to be reflected with the same reflection coefficient as from a sheet admittance in free-space.

Now, on extending this concept to model the three-dimensional artificial material as a periodically loaded transmission line, the appropriate loads to the transmission line correspond to the equivalent sheet

admittances of the elementary planes. In the wire medium, all the elementary planes have the same value of sheet admittance, Y_{sh} . Application of Floquet's theorem [22, Sec. 9.1] to the analysis of the periodically loaded transmission line [32] determines the complex (Bloch) propagation constant $\gamma = j\kappa$ that solves⁶ the transcendental equation [30, p. 367]

$$\cosh(\gamma D_x) = \cos(k_o s_x D_x) + \frac{j}{2} \eta_o Y_{\text{sh}} \left(\frac{1 - s_z^2}{s_x} \right) \sin(k_o s_x D_x) \quad (6)$$

and also the effective (Bloch) impedance Z_x (referred to the midpoint between two adjacent elementary planes) [22, p. 369]

$$Z_x = Z_{\text{TM}} \sqrt{\frac{2 \sin(k_o s_x D_x) - j Y_{\text{sh}} Z_{\text{TM}} [\cos(k_o s_x D_x) - 1]}{2 \sin(k_o s_x D_x) - j Y_{\text{sh}} Z_{\text{TM}} [\cos(k_o s_x D_x) + 1]}} \quad (7)$$

where $Z_{\text{TM}} = \eta_o (1 - s_z^2) / (s_x)$ and D_x is the physical length of transmission line between any two adjacent shunt admittance loads (corresponding to the distance D_x between elementary planes in the artificial material). We notice here, of course, that the propagation constant and transverse impedance are both functions of Y_{sh} .

5 Effective media limit

When $k_o s_x D_x$ and κD_x are small, then the effective wavenumber and impedance of the periodically-loaded transmission line should reduce to that of homogeneous transmission line with some additional per unit length shunt loading of Y_{sh}/D_x . In this limit, the unbounded wire medium can be macroscopically considered as a *homogeneous anisotropic medium* in which the z -component of diagonal relative *equivalent*⁷ permittivity is different from unity and the other two components are nearly unity. To make the connection

⁶As is well known, there are additional, higher order, spatial harmonics that also solve (6); these are given by $\kappa_n = \kappa + 2\pi n/D_x$. Here we only consider the fundamental mode.

⁷The adjective *equivalent* is used to denote that in the effective media limit the wire medium can be macroscopically viewed as a *medium* with an *equivalent* effective permittivity tensor when considering wave propagation. Such permittivity does not have the complete meaning and role of the conventional permittivity or *dielectric constant* obtained phenomenologically for a dielectric.

between the periodic structure parameters and effective media parameters, consider making the appropriate small argument approximations to find:

$$\gamma = j\kappa \rightarrow j\kappa_e = jk_0s_x \sqrt{1 - \frac{jY_{\text{sh}}Z_{\text{TM}}}{k_0s_xD_x}} \quad (8)$$

$$Z_x \rightarrow Z_{xe} = \frac{Z_{\text{TM}}}{\sqrt{1 - \frac{jY_{\text{sh}}Z_{\text{TM}}}{k_0s_xD_x}}}. \quad (9)$$

The wavenumber κ_e defined in (8), like κ , is only the x -component of the total vector wavenumber.⁸ Since the equivalent sheet admittance is purely imaginary (i.e., $Y_{\text{sh}} = jB_{\text{sh}}$), the argument of the square root is real; if the susceptance is capacitive, the wire medium appears to allow propagation of waves with κ_e (real) such that $\kappa_e > k_0s_x$ (hence, the index of refraction for the x -component of wavenumber of the wire medium is greater than unity). On the other hand, if the susceptance is inductive ($0 > -jY_{\text{sh}} > -k_0s_xD_x/Z_{\text{TM}}$), the wire medium may allow propagation of waves with $\kappa_e < k_0s_x$, or, if $\mathcal{I}\{Y_{\text{sh}}\}$ is sufficiently negative (i.e., if $-jY_{\text{sh}} < -k_0s_xD_x/Z_{\text{TM}}$), then with purely real γ , indicating the wave is evanescent (in the x -direction). Effective media theory is a reasonable substitute for periodic structure theory if one can ensure operation of the material near the central axis of the band diagrams in the periodic structure; clearly, effective media theory cannot reproduce the standard stop-band behavior that occurs near the band-edges of a periodic structure.

To compute the equivalent effective permittivity of unbounded wire media, we assume a relative permittivity tensor given by $\bar{\epsilon} = \epsilon_{xx}\hat{x}\hat{x} + \epsilon_{yy}\hat{y}\hat{y} + \hat{y} + \epsilon_{zz}\hat{z}\hat{z}$. Owing to the thinness of the wires, the induced polarization across the cross section is negligible and thus we can take $\epsilon_{xx} = \epsilon_{yy} = 1$ (see Footnote 2). However, from the effective wavenumber (8) and effective transverse impedance (9), one can deduce (recall

⁸The y and z components of the vector wavenumber are the same as those components of the incident vector wave number.

$$Y_{\text{sh}} = jB_{\text{sh}})$$

$$\epsilon_{zz} = 1 + \frac{B_{\text{sh}}\eta_o}{k_o D_x} \quad (10)$$

reflecting the effective loading of the material by the wires. Here, if $B_{\text{sh}} > 0$ (i.e., capacitive loading), then the equivalent relative permittivity ϵ_{zz} is greater than unity; if $0 > B_{\text{sh}} > -k_o D_x / \eta_o$, then the equivalent relative permittivity ϵ_{zz} is less than unity; and, if $B_{\text{sh}} < -k_o D_x / \eta_o$, then the equivalent relative permittivity ϵ_{zz} is negative. Since B_{sh} is always real (for loss-less wires), the equivalent relative permittivity is also always real. The idea of refractive indices less than unity was also observed by Brown in his investigation of the rodged media [26] and by Bahl and Gupta [38]. It is interesting to note that the possibility of a negative component of tensorial equivalent permittivity may lead to some of the features discussed by Felsen and Marcuvitz [39, Sec. 7.1, 7.3] in connection with modeling a cold plasma under the influence of a strong axial magnetic field. Furthermore, because B_{sh} is a function of angle of incidence, the *equivalent* relative permittivity depends upon the angle of incidence and frequency (as well as upon the physical parameters of the media). Consequently, wire media appears spatially dispersive, with the equivalent medium parameters depending upon the vector wavenumber of the propagating wave.

In order to ascertain the characteristics of wave propagation in wire media, we suppose a plane wave in free-space encounters a semi-infinite wire medium that occupies the region $x > 0$. Taking the z direction to be the axes of all the parallel wires and the interface between free-space and the wire medium to be in the $y - z$ plane, then the incident wave can be decomposed into its TE^z and TM^z constituent waves. The TE^z portion does not appreciably interact with the wire medium, so the transmitted TE^z portion is $\mathbf{E}^{(\text{tran}),\text{TE}}(x) \approx \mathbf{E}^{(\text{inc}),\text{TE}}(x)$. On the other hand, the TM^z portion does interact with the medium, bringing about a reflected wave in the vacuum region outside the wire medium. The reflection coefficient can be calculated based on the transverse input impedance of the periodic structure as given by $R_{\text{TM}} = \frac{Z_x - Z_{\text{TM}}}{Z_x + Z_{\text{TM}}}$, where $Z_{\text{TM}} = \eta_o(1 - s_z^2)/(s_x)$ is the transverse wave impedance of a TM^z wave outside the wire medium.

6 Results and Discussion

Having now presented the underlying theory associated with our analysis of wire media, we now turn to a few illustrative examples. For a larger set of examples, the reader is referred to [32]. In particular, we show results for a specific case of wire media constructed from gangbuster surfaces with the parameters listed in Figure 1. The order of the figures is intended to illustrate the general procedure outlined above, beginning with the single elementary plane reflection coefficient and sheet admittance, continuing with the medium parameters (wavenumber and transverse impedances), and finishing with the z -component of the equivalent effective (tensorial) permittivity. Along the way we also show an interesting figure regarding the direction of (phase) propagation within a wire medium half-space as a function of angle of incidence. In our studies we noticed that the variation of these parameters was greater as a function of incidence angle in the E-plane (x - z plane) than in the H-plane (x - y plane), so we have restricted the incident wave to lie in the E-plane for the results presented here. Additionally, we only consider TM^z waves in this section; as mentioned earlier, the wire medium is essentially transparent to TE^z waves.

6.1 Reflection coefficient of a single elementary plane

In Figure 3a the surface reflection coefficient is plotted as a function of increasing λ_o/Λ (i.e., increasing relative wavelength) for a normally incident TM^z plane wave. At the smallest relative wavelength, $\lambda_o/\Lambda = 0.25$, the wires in the array are just over two wavelengths long (i.e., $L = 2.13 \lambda_o$) and, at the largest relative wavelength, $\lambda_o/\Lambda = 2$, the wires in the array are just over a quarter wavelength long (i.e., $L = 0.27 \lambda_o$). Grating lobes are not present for normal incidence throughout this range of relative wavelengths. Three features of this plot, which are typical for frequency selective surfaces, are especially striking. First, notice two points on the curve where the reflection coefficient indicates the gangbuster surface is essentially completely reflecting ($R = -1$): one occurs for $\lambda_o/\Lambda = 0.83$ (i.e., $L = 0.64 \lambda_o$), the other for $\lambda_o/\Lambda = 0.34$ (i.e., $L = 1.57 \lambda_o$). Second, notice the deep null in the reflection that occurs near $\lambda_o/\Lambda = 0.39$ (i.e., $L = 1.37 \lambda_o$), between the two points of complete reflection. This is a feature of devices exhibiting multiple resonances and has been

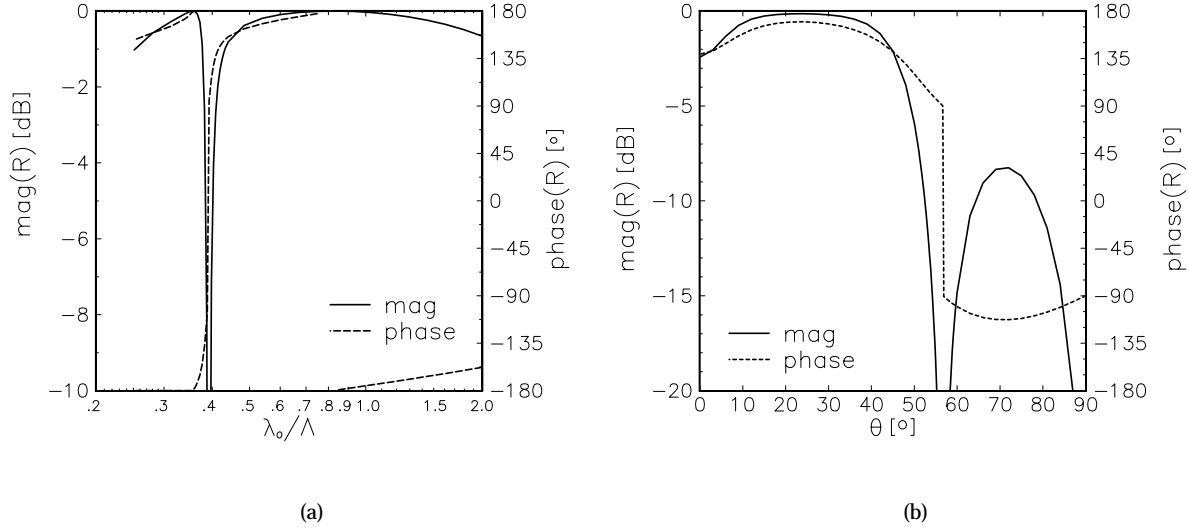


Figure 3: A plot of (a) the (compensated) reflection coefficient as a function of normalized wavelength for normally incident TM^z plane waves on the example gangbuster surface (see Figure 1); (b) the E-plane specular plane wave reflection coefficient as a function of incidence angle for a single gangbuster surface illuminated with incident wavelength $\lambda_o = 0.41\Lambda$. The parameters for this gangbuster surface are given in Figure 1.

given the name *modal interaction null* in the literature [34]. On fixing the wavelength of the incident wave to $\lambda_o = 0.41\Lambda$ and varying the angle of incidence in the E-plane (set $s_x = \cos \theta$, with θ the angle of incidence to the elementary plane), we notice in Figure 3b somewhat similar features as in Figure 3a. Although the surface does not become perfectly reflecting for any angle of incidence, the reflection coefficient is large for angles near normal incidence (θ near 0) and then vanishes near $\theta = 57^\circ$ and again for $\theta = 90^\circ$ (grazing incidence).

6.1.1 Equivalent sheet reactance

Next we use the reflection data presented above to compute the equivalent surface admittance. Since the surface is loss-less, the admittance is purely imaginary; instead of presenting B_{sh} , we have plotted $X_{\text{sh}} = -1/B_{\text{sh}}$. At the two points where the surface is completely reflecting, the array is resonant, as can be seen by interpreting Figure 4a for the equivalent sheet reactance of the surface. At these points, the sheet reactance vanishes, indicating, as in lumped circuits, that the time-averaged stored electric and magnetic energies are equal. In between the two resonances, at the modal interaction null, the sheet reactance is infi-

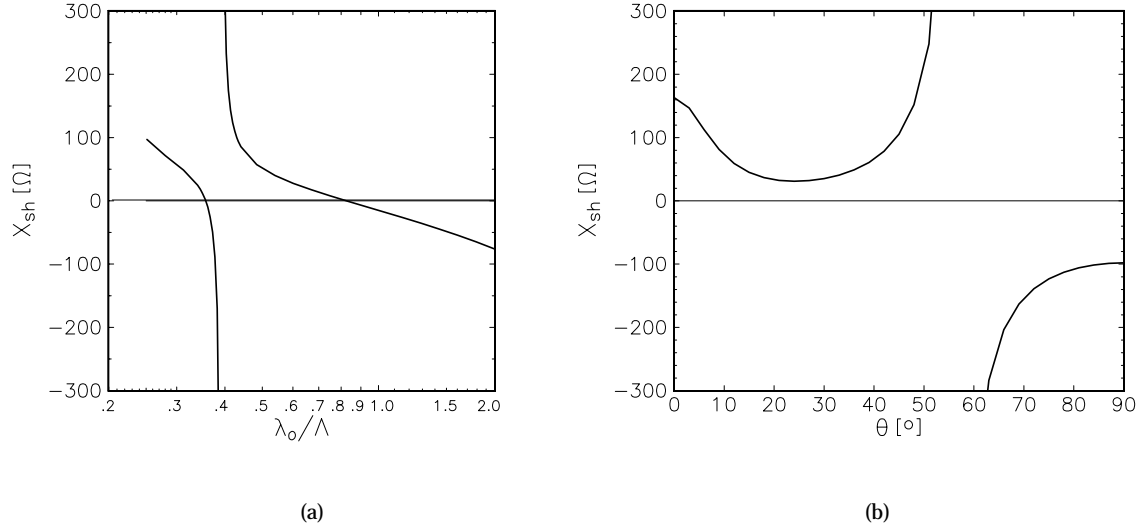


Figure 4: A plot of (a) the imaginary part of the sheet impedance $Z_{\text{sh}} = 1/Y_{\text{sh}} = R_{\text{sh}} + jX_{\text{sh}}$ as a function of normalized wavelength for TM^z normal incidence on the example gangbuster surface; (b) The sheet reactance as a function of incidence angle (in the E-plane) for a single gangbuster surface illuminated with incident wavelength $\lambda_o = 0.41\Lambda$. Since the sheet impedance is purely reactive, the real part of Z_{sh} vanishes ($R_{\text{sh}} = 0$), so only the imaginary part is shown. The parameters for the gangbuster surface are given in Figure 1.

nite, implying there is no “equivalent average uniform surface current” and thus there can be no scattered waves—all of the incident power is transmitted. Notice that for long wavelengths the sheet reactance is negative (this corresponds to the well-known fact that dipoles excited below resonance have a capacitive input impedance); for wavelengths between the first resonance and the modal interaction null, the sheet reactance is positive (corresponding to the inductive input impedance of dipoles excited just above resonance); for wavelengths between the modal interaction null and the second resonance, the sheet reactance is again capacitive, due to the strong excitation of the second current mode. Finally, for those wavelengths (shown in the figure) shorter than the wavelength of the second resonance, the sheet reactance is again inductive. If this plot were extended to even shorter wavelengths, we would expect to see a similar trend of alternation of zeros and poles in the sheet reactance. Notice, the resonances appear roughly near the *odd* multiples of a half wavelength; since the array (for the examples of Figures 3a and 4a) is excited by a normally incident plane wave, odd current modes are not excited on the wires and so there are no resonances near the even multiples of a half wavelength. Analogous to Figure 3b, the sheet reactance is plotted in Figure 4b as a function of angle of incidence in the E-plane for fixed wavelength $\lambda_o = 0.41\Lambda$. Notice that at the

incidence angle for which the equivalent sheet reactance is infinite, the reflection coefficient (see Figure 3b) vanishes. For large angles of incidence, the equivalent reactance is negative (i.e., the surface appears to have a capacitive nature) and for smaller angles of incidence, the equivalent reactance is positive (i.e., the surface appears inductive). One can expect then, that when these elementary planes are used to create a medium, if the equivalent reactance is negative, then the medium might behave as if it were capacitively loaded; on the other hand, if the equivalent reactance is positive, then the medium might behave as if it were inductively loaded. This variation of X_{sh} as a function of angle of incidence is responsible, in part, for giving rise to the spatially-dispersive behavior of wire media.

6.2 Wire media

Suppose the gangbuster surface discussed here is used as the elementary planes of a wire medium. The elementary planes, with interplanar spacing D_x , should be placed far enough apart that the evanescent waves of neighboring planes do not significantly interact but close enough that the period is a small fraction of a wavelength. It has been noted (see, for example [22, p. 773]) that, as a rule of thumb, if the neighboring planes are spaced far enough apart that the first evanescent wave (in the plane-wave expansion) excited at an elementary plane decays at least 20 dB (compared to the propagating wave) through a distance D_x , then all of the evanescent waves can be discarded. For the values of λ_o , D_x , and D_τ used in these examples, we find that the first evanescent wave has decayed by at least 28 dB for all ratios of λ_o/Λ examined. In the plots shown below, the inter-planar spacings are chosen as $D_x = \Lambda/15$; as can be seen in Figure 5 the normalized x -component of wavenumber, κ/k_o , of the periodic wave (recall from Footnote 6 that we are only considering the principal value, or dominant mode solution to (6)) is purely real for long relative wavelength (roughly, $\lambda_o/\Lambda \gtrsim 1.3$), but as the wavelength decreases, the x -component of the wavenumber becomes complex ($0.8 \lesssim \lambda_o/\Lambda \lesssim 1.3$), and is eventually purely imaginary ($0.4 \lesssim \lambda_o/\Lambda \lesssim 0.8$). As the wavelength continues to decrease, one may speculate that this progression repeats (and also that the bandgap effects of the periodic lattice may appear). Also, we have plotted the corresponding x -component of wavenumber as determined by the effective media theory (Equation 8); here we see certain ranges for which the effective

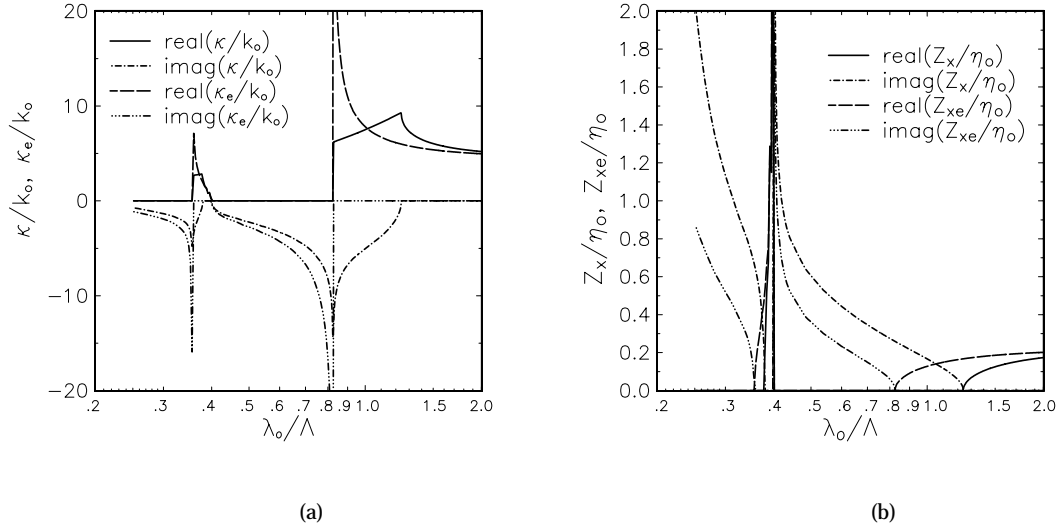


Figure 5: A plot of (a) the normalized x -component of wavenumber, κ/k_0 , of the periodic wave and its effective-media counterpart κ_e/k_0 (see Footnote 6) and (b) the transverse impedance of both waves as functions of relative wavelength for a wire medium conceptually constructed from layers of gangbuster surfaces separated by an inter-planar distance of $D_x = \Lambda/15$ (see Footnote 9). Each gangbuster surface is identical—the parameters are given in Figure 1. Physical remarks are given in the text.

media theory may apply (based on the similarity of results for the periodic and effective media theories), and other ranges—especially where κ is complex—where it may not. Clearly, if one allows D_x to decrease (but not beyond the point where the interaction of the evanescent waves is significant), then the results of the effective media theory and the periodic theory would be closer. Figure 5b shows the two transverse impedances associated with these wavenumber.⁹ As can be seen, in the regions where the wavenumber are purely imaginary, so too is the transverse impedance (as one would expect).¹⁰

We can understand the differences between the regions of real, imaginary, and complex κ by noting the value of equivalent sheet reactance in each region. In the first region, the sheet reactance (see Figure 4) is large and negative—this implies the x -component of wavenumber will be purely real. In the second region, the sheet reactance is small and negative; here $k_0 s_x D_x = \pi$ indicates that the wave is experiencing the bandgap effect of periodic media. As is well known in the analysis of wave propagation in periodic structures, complex effective wavenumber may occur in these bandgap regions. In such regions, there is

⁹The transverse impedance for the wave associated with the wavenumber κ is evaluated at the midpoint between the adjacent elementary planes.

¹⁰Because of the granularity of the data, it appears that at certain points the impedance might be complex, however this is only a plotting artifact. The transverse impedance is either purely real or purely imaginary.

significant coupling between the traveling wave and the backward wave and so the energy of the forward wave is mainly transferred into the backward wave. For this reason, the effective media approximations are not valid in these regions and the full periodic media approach must be employed. Continuing, in the third region, when the sheet reactance becomes positive, the x -component of wavenumber is now purely imaginary. In this region evanescence is not due to band-gap phenomena, but instead to the heavily inductive loading of the medium. Both effective media theory and periodic structure theory are applicable for this region.

Do these properties remind us of photonic bandgap structures? It must be noted that the evanescent regions, where the normal component (i.e., x -component) of the wavenumber is purely imaginary, are not due to the conventional bandgap features of periodic structures, since the elementary planes are closely spaced ($D_x = \Lambda/15$). Rather it is mainly due to the properties of the currents induced on each elementary plane and their resulting effect of shunt loading on the wave propagating in the medium. Since the spacing between the elementary planes is smaller than that for typical photonic bandgap structures, more compact wire media can be designed to provide some of the features of photonic band-gap structures.

Next, in Figure 6, the x -component of vector wavenumber is plotted (also for $D_x = \Lambda/15$). In these figures, when the incident angle is greater than approximately $\theta = 52^\circ$, the curves corresponding to effective media theory and periodic structure theory essentially overlap, while for smaller incident angles the two theories seem to agree less. As can be seen in these figures for this example of wire media, the plane wave cannot penetrate into the medium for angles of incidence in the E-plane between $\theta = 0$ and $\theta = 52^\circ$. Notice that for near normal incidence, plane waves cannot penetrate into the wire medium (the normal component of wavenumber inside the wire medium is purely imaginary; i.e., the transmitted wave is evanescent) and thus the incident power will be totally reflected at the interface. However, the wavenumber in the z direction is real (as phase-matching requires for oblique incidence), so the wave is essentially an inhomogeneous plane wave—the phase progresses in the z direction, yet the amplitude decays in the x direction. This phenomenon, although perhaps expected, is an interesting characteristic and is rather *opposite* to what usually occurs in the case of conventional total internal reflection for which the wave is totally reflected for

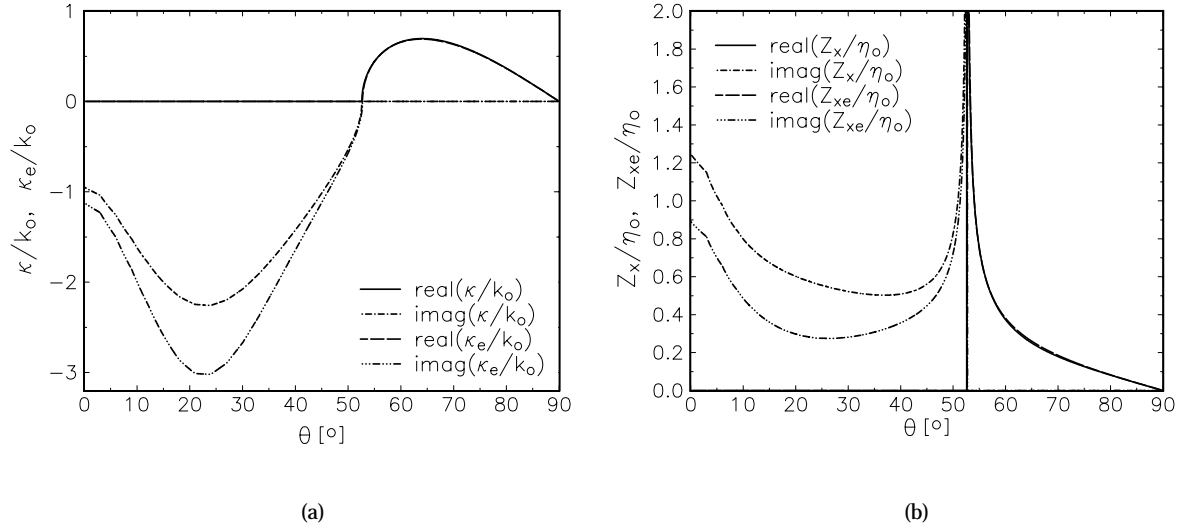


Figure 6: A plot of (a) the normalized x -component of wavenumber, κ/k_0 , of the periodic wave and its effective media counterpart κ_e/k_0 (see Footnote 6 and (b) the transverse impedance of both waves for a wire medium conceptually constructed from layers of gangbuster surfaces separated by an inter-planar distance of $D_x = \Lambda/15$ (see Footnote 9). Each surface is identical—the parameters are given in Figure 1. The plot shows both the real and imaginary parts as a function of incidence angle θ in the E-plane ($s_y = 0$; $s_x = \cos \theta$) for an incident wave of wavelength $\lambda_o = 0.41\Lambda$. Here, θ is the angle of incidence of an illuminating wave to an interface between vacuum and a semi-infinite wire medium, with $\theta = 0$ corresponding to normal incidence and $\theta = 90^\circ$ corresponding to grazing incidence. Physical remarks are given in the text.

angles of incidence between grazing incidence and some critical angle. This rather unusual property of wire media, when combined with the usual feature of total internal reflection between two unequal dielectrics, may find some useful application in the design of novel waveguiding structures.

To support our arguments for the direction of propagation inside the wire medium as a function of the angle of illumination of the incident wave, we show in Figure 7a the interior angle of propagation, θ_{med} , as a function of the angle of incidence, θ . When $0 < \theta \lesssim 52^\circ$, there is no propagation into the wire medium on account of purely imaginary κ (and κ_e). As θ increases to angles of incidence greater than approximately 52° , the wave begins to propagate within the wire medium parallel to the interface ($\theta_{\text{med}} = 90$) and then peaks at some oblique angle $\theta_{\text{med}} \approx 51^\circ$. As θ continues to increase, the wave inside the wire medium returns to make a grazing angle to the interface. Therefore, plane wave propagation within the wire medium for TM^z E-plane incidence is restricted to an “angular window” about the z -axis (grazing incidence). The component of the equivalent effective permittivity ϵ_{zz} (see Equation 10) is plotted in Figure 7b for the wire medium considered here. This permittivity is the equivalent effective permittivity

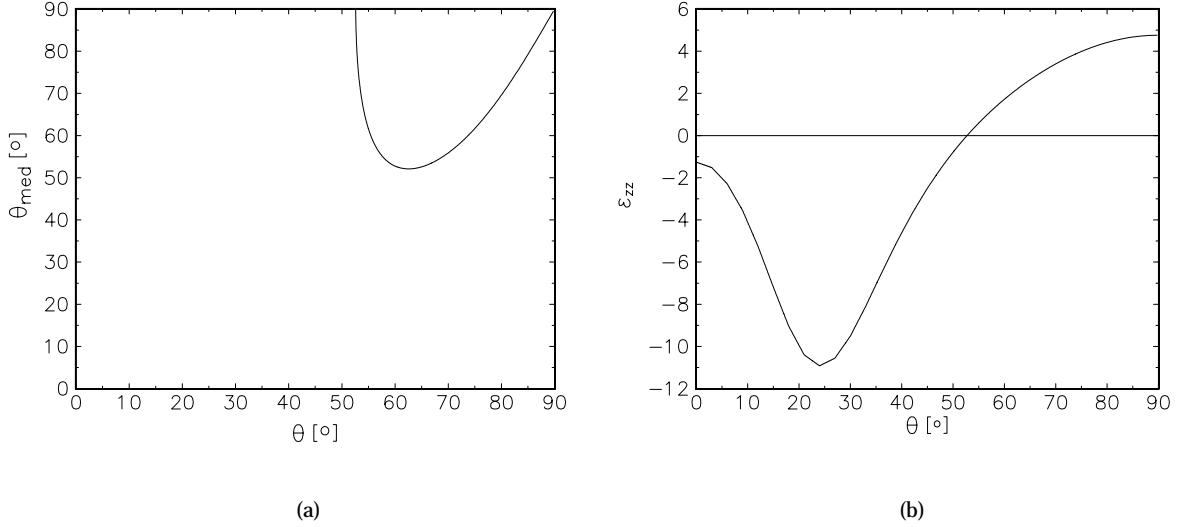


Figure 7: Plots of (a) the propagation angle, θ_{med} , in a wire medium as a function of the angle of incidence, θ , in the E-plane and (b) z -component of equivalent (see Footnote 7) effective relative permittivity, ϵ_{zz} , for the wire medium considered here as a function of the angle of incidence in the E-plane for an incident wave of wavelength $\lambda_o = 0.41\Lambda$ and an inter-planar spacing of $D_x = \Lambda/15$. The parameters for the gangbuster surface are given in Figure 1.

of the wire medium when it can be considered as a homogeneous medium (see Footnote 7). Notice, in the region where wave propagation is permitted within the wire medium, ϵ_{zz} is positive; in the other region, it is negative. Felsen and Marcuvitz [39, Sec. 7.1] considered the case of a uniaxial dielectric with ϵ_z (their notation) negative and found that such media prohibits wave propagation in certain angular regions. A similar mechanism may be responsible for wave behavior here.

Based on our theoretical analysis reported here and in [32], wire media possess interesting spatial dispersion characteristics, *viz.*, with appropriate design parameters (number densities, orientation, and length of the simple wire inclusions) these media, even though loss-less, may exhibit *wave windowing*, i.e., they may prohibit wave propagation in certain directions while allowing propagation in other directions. Furthermore, these media are frequency dependent and behave differently for different polarizations. In other words, like frequency-selective surfaces and filters, wire media may effectively behave as angle-selective volumes and filters, frequency-selective volumes and filters, and polarization-selective volumes and filters. Such properties may find interesting applications; for example, in beam-forming for small antennas embedded in wire media or as radomes for selecting directions, polarizations, and frequencies of radiation.

Even though the wires of wire media seem to be densely packed on each elementary plane, the volume fraction is still very small (less than 0.15% for the example presented) since the radius of the wires is taken to be small. Despite the small volume fraction of the metal inclusions, the resulting medium may have significantly different electromagnetic properties than the host medium alone. If one compares two blocks of dielectric—one with wire inclusions and the other without—substantial differences in the electromagnetic properties will be noticed. This change in electromagnetic properties of the material may have very useful applications for design of antennas, devices and components. Moreover, the mechanical structures of such media are rather simple, so one may speculate that these media might be constructed with the use of microfabrication and micromachining technologies.

In our analysis, we have only considered plane wave propagation in wire media. However, it is also interesting to note how one might determine the electromagnetic fields arising due to sources present in such media. In order to synthesize source-excited fields, one can express them in terms of a plane wave spectrum (i.e., spatial Fourier transform), and then determine the interaction of each of these plane waves with the wire medium. One will need to perform an inverse transform if results in the original domain are desired. If, in this inverse transformation, one needs to deform the contour of integration into the complex angular domain, since the plane wave spectra in this medium are not represented in terms of closed-form expressions, the analytic continuation for the wavenumber would not be obviously tractable. However, if one considers propagation of Gaussian waves (which includes elements of the plane wave spectrum in the desired direction of propagation as well as those in other directions with appropriate weighting functions), then most of the contribution to the inverse transformation integral would arise near the wavenumber corresponding to the direction of the Gaussian beam. This being the case, if one is satisfied with numerical integration of the inverse transform, then one may avoid integration along the entire axis of the complex angular domain and instead consider the major contributions to the integral that appear near the wavenumber of the Gaussian wave. Of course one would need to know (albeit numerically) the plane wave spectra for all wavenumber in order to evaluate such integrals completely. It must also be noted that the reciprocity theorem can be applied as an alternative technique for finding the far-zone fields of a radiating dipole in

such a medium (see, e.g., Section III, Ref. 40). Finally, the idea that an artificial material can be divided into a number of elementary planes for analysis can also be used as a general synthesis principle. Then, any of the well-known types of surfaces that display interesting behavior (e.g., frequency selective surfaces or polarization selective surfaces) can be used as basic building blocks for artificial material.

References

- [1] I. V. Lindell, A. H. Sihvola, and J. Kurkijärvi, "Karl F. Lindman: The last Hertzian, and a harbinger of electromagnetic chirality," *IEEE Antennas and Propagation Magazine*, vol. 34, no. 3, pp. 24–30, June 1992.
- [2] W. E. Kock, "Metallic delay lenses," *Bell Systems Technical Journal*, vol. 27, pp. 58–82, 1948.
- [3] A. Ishimaru, *Electromagnetic wave propagation, radiation, and scattering*, Prentice Hall, Englewood Cliffs, 1991.
- [4] W. R. Tinga, "Mixture laws and microwave-material interactions," in *Progress in Electromagnetic Research (PIER) Monograph Series Vol. 6 on Dielectric Properties of Heterogeneous Materials*, A. Priou, Ed., chapter 1, pp. 1–40. Elsevier, New York, 1992.
- [5] J. Brown, "Artificial dielectrics," in *Progress in Dielectrics, Vol. 2*, J. B. Birks and J. H. Schulman, Eds., pp. 193–225. Heywood, London, 1960.
- [6] A. F. Harvey, "Optical techniques at microwave frequencies," *Proceedings of the Institution of Electrical Engineers*, vol. 106, Part B, pp. 141–157, 1959.
- [7] D. F. Sievenpiper, M. E. Sickmiller, and E. Yablonovitch, "3D wire mesh photonic crystals," *Physical Review Letter*, vol. 76, no. 14, pp. 2480–2483, April 1996.
- [8] J. Brown and W. Jackson, "The properties of artificial dielectrics at centimetre wavelengths," *Proceedings of the IEE*, vol. 102B, pp. 11–21, 1955.
- [9] D. L. Jaggard, A. R. Mickelson, and C. H. Papas, "On electromagnetic waves in chiral media," *Journal of Applied Physics*, vol. 18, pp. 211–216, 1979.
- [10] I. P. Theron and J. H. Cloete, "The optical activity of an artificial non-magnetic uniaxial chiral crystal at microwave frequencies," *Journal of Electromagnetic Waves and Applications*, vol. 10, pp. 539–561, 1996.
- [11] D. L. Jaggard and N. Engheta, "Chirality in electrodynamics: Modeling and applications," in *Directions in Electromagnetic Wave Modeling*, H. L. Bertoni and L. B. Felsen, Eds. Plenum, New York, tent. 1991, Bibliographic information taken from preprint.
- [12] S. A. Tretyakov, R. Mariotte, C. R. Simovski, T. G. Kharina, and J. Heliot, "Analytical antenna model for chiral scatterers: comparison with numerical and experimental data," *IEEE Transactions on Antennas and Propagation*, vol. 44, pp. 1006–1014, 1996.
- [13] A. Cherepanov and A. Sihvola, "Internal electric field of anisotropic and bianisotropic spheres," *Journal of Electromagnetic Waves and Applications*, vol. 10, pp. 79–91, 1996.
- [14] L. R. Arnaut, "Interaction between bianisotropic particles," *Journal of Electromagnetic Waves and Applications*, vol. 11, pp. 133–137, 1997.
- [15] A. J. Bahr and K. R. Clausing, "An approximate model for artificial chiral material," *IEEE Transactions on Antennas and Propagation*, vol. 42, pp. 1592–1599, 1994.

- [16] K. W. Whites, “Full-wave computation of constitutive parameters for loss-less composite chiral materials,” *IEEE Transactions on Antennas and Propagation*, vol. 43, pp. 376–384, 1995.
- [17] M. M. I. Saadoun and N. Engheta, “Theoretical study of electromagnetic properties of non-local Ω media,” in *Progress in Electromagnetic Research (PIER) Monograph Series Vol. 9 on Bianisotropic and Bi-Isotropic Media and Applications*, A. Pirou, Ed., chapter 15, pp. 351–397. EMW Publishing, Cambridge, MA, 1994.
- [18] R. Luebbers, H. S. Langdon, F. Hunsberger, C. F. Bohren, and S. Yoshikawa, “Calculation and measurement of the effective chirality parameter of a composite chiral material over a wide frequency band,” *IEEE Transactions on Antennas and Propagation*, vol. 43, pp. 123–129, 1995.
- [19] G. Oberschmidt and A. F. Jacob, “Averaging rules for the scattering by randomly oriented chiral particles,” *IEEE Transactions on Microwave Theory and Techniques*, vol. 44, pp. 476–478, 1996.
- [20] A. H. Sihvola and L. V. Lindell, “Analysis on chiral mixtures,” *Journal of Electromagnetic Waves and Applications*, vol. 6, pp. 553–572, 1992.
- [21] S. A. Tretyakov and F. Mariotte, “Maxwell Garnett modeling of uniaxial chiral composites with bianisotropic inclusions,” *Journal of Electromagnetic Waves and Applications*, vol. 9, pp. 1011–1025, 1995.
- [22] R. E. Collin, *Field Theory of Guided Waves*, IEEE Press, New York, 1991.
- [23] J. L. Blanchard, E. H. Newmann, and M. E. Peters, “Integral equation analysis of artificial media,” *IEEE Transactions on Antennas and Propagation*, vol. 42, pp. 727–731, 1994.
- [24] M. E. Peters and E. H. Newmann, “Method of moments analysis of anisotropic artificial media composed of dielectric wire objects,” *IEEE Transactions on Microwave Theory and Techniques*, vol. 43, pp. 2023–2027, 1995.
- [25] S. Singh and R. Singh, “Application of transforms to accelerate the summation of periodic free-space green’s functions,” *IEEE Transactions on Microwave Theory and Techniques*, vol. 38, no. 11, pp. 1746–1748, November 1990.
- [26] J. Brown, “Artificial dielectrics having refractive indices less than unity,” *Proceedings of the IEE*, vol. 100, pt. 4, pp. 51–62, 1953.
- [27] C. A. Moses and N. Engheta, “An idea for electromagnetic feedforward-feedbackward media,” Accepted for publication in *IEEE Transactions on Antennas and Propagation*, to appear in April 1999 issue.
- [28] R. Mittra, C. H. Chan, and T. Cwik, “Techniques for analyzing frequency selective surfaces—a review,” *Proceedings of the IEEE*, vol. 76, pp. 1593–1615, 1988.
- [29] B. A. Munk and G. A. Burrell, “Plane-wave expansion for arrays of arbitrarily oriented piecewise linear elements and its application in determining the impedance of a single linear antenna in a lossy half-space,” *IEEE Transactions on Antennas and Propagation*, vol. AP-27, pp. 331–343, 1979.
- [30] R. E. Collin, *Foundations for Microwave Engineering*, Mc-Graw Hill, New York, 1966.
- [31] C. Moses and N. Engheta, “Theoretical electromagnetic modeling of non-local-coupled-dipole artificial dielectric — preliminary results,” in *Symposium Digest of the Fourteenth Annual Benjamin Franklin Symposium on New Frontiers in Antenna and Microwave Technology*, Philadelphia, May 3 1996, pp. 92–93.
- [32] C. A. Moses, *A theoretical study of electromagnetic feedforward/feedbackward media and wire media*, Ph.D. thesis, University of Pennsylvania, 1998.

- [33] S. W. Schneider and B. A. Munk, "The scattering properties of "super dense" arrays of dipoles," *IEEE Transactions on Antennas and Propagation*, vol. 42, pp. 463–472, 1994.
- [34] C. J. Larson and B. A. Munk, "The broad-band scattering response of periodic arrays," *IEEE Transactions on Antennas and Propagation*, vol. AP-31, pp. 261–267, 1983.
- [35] T. W. Kornbau, *Analysis of periodic arrays of rotated linear dipoles, rotated crossed dipoles, and biplanar dipole arrays in dielectric*, Ph.D. thesis, The Ohio State University, 1984.
- [36] W. L. Stutzman and G. A. Thiele, *Antenna Theory and Design*, Wiley, New York, 1981.
- [37] A. Carne and J. Brown, "Theory of the reflections from the rodged-type artificial dielectric," *Proc. Inst. Elect. Engrs*, vol. 106 Part B, pp. 107–115, 1959.
- [38] I. J. Bahl and K. C. Gupta, "A leaky-wave antenna using an artificial dielectric medium," *IEEE Transactions on Antennas and Propagation*, vol. 22, pp. 119–122, 1974.
- [39] L. B. Felsen and N. Marcuvitz, *Radiation and Scattering of Waves*, IEEE Press, New York, 1994.
- [40] N. G. Alexopoulos and D. R. Jackson, "Fundamental superstrate (cover) effects on printed circuit antennas," *IEEE Transactions on Antennas and Propagation*, vol. AP-32, no. 8, pp. 807–816, August 1984.